

# Activation and intrinsic $\gamma$ -secretase activity of presenilin 1

Kwangwook Ahn<sup>a</sup>, Christopher C. Shelton<sup>a,b</sup>, Yuan Tian<sup>a,c</sup>, Xulun Zhang<sup>d</sup>, M. Lane Gilchrist<sup>a,e</sup>, Sangram S. Sisodia<sup>d</sup>, and Yue-Ming Li<sup>a,b,1</sup>

<sup>a</sup>Molecular Pharmacology and Chemistry Program, Memorial Sloan-Kettering Cancer Center, New York, NY 10065; <sup>b</sup>Department of Pharmacology, <sup>c</sup>Department of Physiology, Biophysics and Systems Biology, Weill Graduate School of Medical Sciences of Cornell University, New York, NY 10021; <sup>d</sup>Center for Molecular Neurobiology, University of Chicago, Chicago, IL 60637; and <sup>e</sup>Department of Chemical Engineering and Department of Biomedical Engineering, City College of the City University of New York, New York, NY 10031

Edited\* by Don W. Cleveland, University of California at San Diego, La Jolla, CA, and approved October 15, 2010 (received for review September 3, 2010)

**A complex composed of presenilin (PS), nicastrin, PEN-2, and APH-1 is absolutely required for  $\gamma$ -secretase activity in vivo. Evidence has emerged to suggest a role for PS as the catalytic subunit of  $\gamma$ -secretase, but it has not been established that PS is catalytically active in the absence of associated subunits. We now report that bacterially synthesized, recombinant PS (rPS) reconstituted into liposomes exhibits  $\gamma$ -secretase activity. Moreover, an rPS mutant that lacks a catalytic aspartate residue neither exhibits reconstituted  $\gamma$ -secretase activity nor interacts with a transition-state  $\gamma$ -secretase inhibitor. Importantly, we demonstrate that rPS harboring mutations that cause early onset familial Alzheimer's disease (FAD) lead to elevations in the ratio of A $\beta$ 42 to A $\beta$ 40 peptides produced from a wild-type APP substrate and that rPS enhances the A $\beta$ 42/A $\beta$ 40 peptide ratio from FAD-linked mutant APP substrates, findings that are entirely consistent with the results obtained in in vivo settings. Thus,  $\gamma$ -secretase cleavage specificity is an inherent property of the polypeptide. Finally, we demonstrate that PEN2 is sufficient to promote the endoproteolysis of PS1 to generate the active form of  $\gamma$ -secretase. Thus, we conclusively establish that activated PS is catalytically competent and the bimolecular interaction of PS1 and PEN2 can convert the PS1 zymogen to an active protease.**

intermembrane-cleaving proteases | notch | presenilinase | reconstitution

$\gamma$ -Secretase is composed of four proteins: presenilin (PS), Nicastrin (NCT), PEN-2, and APH-1 (1). The observation that ectopic expression of all four polypeptides in *Saccharomyces cerevisiae* can reconstitute enzymatic activity has led to the conclusion that this quartet of proteins is both necessary and sufficient for  $\gamma$ -secretase function (2). While the assembly, stabilization, and trafficking of PS require the presence of APH-1 and NCT, respectively,  $\gamma$ -secretase is “activated” by PEN-2-mediated endoproteolytic cleavage of PS1 within a highly hydrophobic segment encoded by exon 9 of the *PSEN1* gene (3–7). Notwithstanding these important contributions to our understanding of the regulation of  $\gamma$ -secretase, establishing the direct role of each “subunit” in mediating  $\gamma$ -secretase processing of membrane-tethered substrates has been immensely challenging and attempts to do so have led to conflicting results. For example, a mutation of Glu333 in NCT was shown to reduce  $\gamma$ -secretase activity, evidence that was used to support a role of NCT as substrate receptor within the  $\gamma$ -secretase complex (8). In contrast, other studies have reported that the same mutation reduced the formation of the  $\gamma$ -secretase complex (9). Furthermore, a recent report showed the PS1-PEN2-Aph1 complex, in the absence of NCT, is catalytically active under conditions wherein proteasomal degradation is inhibited (10). Clearly, developing an in vitro system that allows reconstitution of  $\gamma$ -secretase activity using purified individual subunits—alone, or in combination—is critical in dissecting the role(s) of these subunits and for elucidation of the reaction mechanism of  $\gamma$ -secretase.

Endoproteolysis of the newly synthesized approximately 52 kDa PS protein to generate amino-terminal (NTF) and carbox-

yl-terminal (CTF) fragments is a critical step for formation of active  $\gamma$ -secretase complexes (9). Previous studies indicated that PS is responsible for  $\gamma$ -secretase activity and endoproteolytic cleavage (termed presenilinase or PSase) because mutagenesis of two putative catalytic residues of PS1 at Asp257 and Asp385 abolished both  $\gamma$ -secretase and PSase activity (11). In addition, it has been reported that PS1 mutations can affect the sites of endoproteolysis (12). On the other hand, Campbell et al. reported that PSase is a membrane-bound aspartyl protease and pharmacologically distinct from  $\gamma$ -secretase (13). Moreover, expression of a catalytically inactive PS molecule that harbors mutations at Asp residues 257 and 385 in PS-deficient cells leads to the production of NTF and CTF, even though the cells remained inactive for  $\gamma$ -secretase activity (14). Thus, there is little consensus as to whether endoproteolysis of PS1 is self-catalyzed or catalyzed by another, as yet characterized, protease.

Despite the ambiguities relevant to the mechanisms of PS endoproteolysis, genetic, biochemical, and cell biological studies have offered support for a role of PS as the catalytic subunit of  $\gamma$ -secretase (11, 15–18). Nevertheless, in every one of these latter instances, PS is coexpressed with other components of the complex, and hence, direct evidence that PS is catalytically active as an independent entity has not yet emerged. In this regard, over 150 PS1 mutations have been described that cause familial Alzheimer's disease (FAD), and in all cases, expression of these PS1 variants both in cultured cells and in vivo leads to elevations in the ratio of pathogenic A $\beta$ 42 to A $\beta$ 40. Our understanding of the interactions of mutant PS and the individual components within the complex and the biochemical mechanism(s) that underlie the alteration in cleavage specificity has been limited by the absence of in vitro reconstitution systems using purified subunits, and we now document a unique experimental system that accomplishes this goal.

In the present study, we report that incorporation of a purified, bacterially synthesized recombinant PS1 (rPS) variant into liposomes exhibits  $\gamma$ -secretase activity that is independent of other components of the complex. Furthermore, we demonstrated that reincorporation of purified, bacterially synthesized recombinant PEN2 is necessary and sufficient for endoproteolysis and activation of PS1. In addition, we demonstrate that rPS harboring mutations that cause early onset FAD lead to elevations in the ratio of A $\beta$ 42 to A $\beta$ 40 produced from a wild-type APP substrate and that rPS enhances the A $\beta$ 42/A $\beta$ 40 peptide ratio from FAD-linked

Author contributions: K.A., M.L.G., S.S.S., and Y.-M.L. designed research; K.A. and M.L.G. performed research; K.A., M.L.G., S.S.S., and Y.-M.L. analyzed data; C.C.S., Y.T., and X.Z. contributed new reagents/analytic tools; and K.A., S.S.S., and Y.-M.L. wrote the paper.

The authors declare no conflict of interest.

\*This Direct Submission article had a prearranged editor.

<sup>1</sup>To whom correspondence should be addressed. E-mail: liy2@mskcc.org.

This article contains supporting information online at [www.pnas.org/lookup/suppl/doi:10.1073/pnas.1013246107/-DCSupplemental](http://www.pnas.org/lookup/suppl/doi:10.1073/pnas.1013246107/-DCSupplemental).

mutant APP substrates in a manner that recapitulates findings in vivo.

## Results

**Reconstituted PS1 $\Delta$ E9-Proteoliposomes Are Catalytically Active.** We exploited a recently developed system that facilitates production of soluble, polytopic membrane proteins (19) in order to express a series of maltose binding protein (MBP)-PS1 chimeras (Fig. 1A). We chose to employ the FAD-linked PS1 $\Delta$ E9 variant as a template, one that lacks the hydrophobic segment containing the endoproteolytic cleavage site and is highly active (18, 20, 21). The consequence of deleting amino acids 290-319 of PS1 to generate the PS1 $\Delta$ E9 molecule results in the substitution of a serine residue at amino acid 290 with cysteine (S290C). Indeed, expression of the S290C variant, rather than the deletion of exon 9, per se, is responsible for the pathological increase in the ratio of A $\beta$ 42:A $\beta$ 40 peptides (21) because reversal of the S290C mutation to wild-type status (C290S) within the PS1 $\Delta$ E9 backbone returned the ratio of A $\beta$ 42:A $\beta$ 40 peptides to wild-type levels (21). Thus, we expressed PS1 $\Delta$ E9 and the PS1 $\Delta$ E9-C290S variant in *Escherichia coli* and developed a procedure for the isolation and reconstitution of these proteins in order to assess  $\gamma$ -secretase activity (Fig. 1B). In parallel, we generated an MBP-PS1 $\Delta$ E9-D385A fusion protein in which aspartate 385, a residue shown to be essential for  $\gamma$ -secretase activity (11), was replaced with alanine. The MBP-PS1 $\Delta$ E9 fusion proteins were purified by affinity chromatography on amylose columns and reconstituted into liposomes in the presence of CHAPS. After detergent removal, the proteoliposomes were treated with thrombin to remove MBP and then further purified by sucrose gradient centrifugation (Fig. 1B). Each of the PS1 $\Delta$ E9 proteins residing in purified proteoliposomes exist as single polypeptides of approximately 52 kDa (Fig. 1C); the identity of these species were confirmed by MS/MS analysis. We

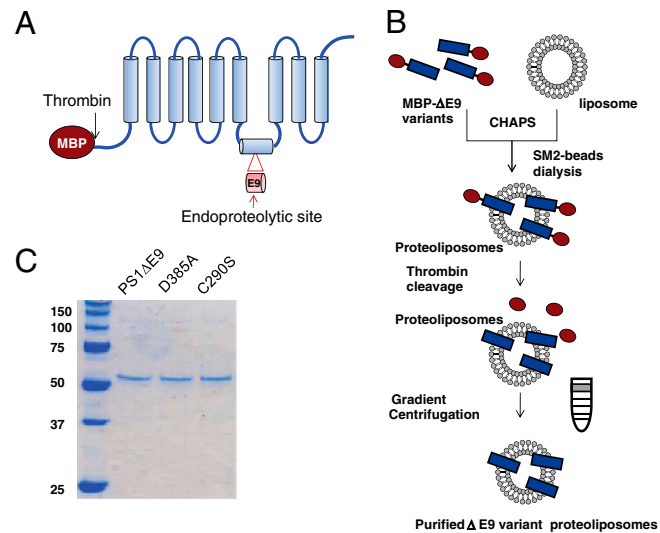


**Fig. 1.** Preparation of proteoliposome containing presenilin exon 9 deletion mutant (PS1 $\Delta$ E9). (A) Diagram of MBP-fused PS1 $\Delta$ E9 protein. The PS1 exon 9 (E9) domain contains the endoproteolytic cleavage site and has been deleted to create PS1 $\Delta$ E9. MBP (maltose-binding protein) has been fused at the N-terminus of PS1 for purification. A thrombin cleavage site has been incorporated between MBP and PS1 $\Delta$ E9 for subsequent MBP removal. (B) Purification and reconstitution procedure for PS1 $\Delta$ E9 insertion into proteoliposomes. MBP-fused PS1 $\Delta$ E9 was overexpressed in *E. coli* and purified using affinity chromatography with an amylose column. The purified MBP-PS1 $\Delta$ E9 protein was introduced into liposomal membranes with CHAPS detergent and reconstituted as a mixture of unincorporated proteins and proteoliposomes after dialysis. Following thrombin removal of the MBP-domain, the end product PS1 $\Delta$ E9 proteoliposome was isolated via sucrose density-gradient centrifugation. (C) Coomassie blue staining of purified proteins that were isolated after thrombin cleavage and density-gradient centrifugation.

determined that lipid mixture of eggPC:total brain lipid extract at a ratio of 70:30 (w/w) was found to be optimal for PS1 $\Delta$ E9-proteoliposome-derived  $\gamma$ -secretase activity (Fig. S1A). The purified PS1 $\Delta$ E9-proteoliposomes were incubated with a biotinylated recombinant APP substrate Sb4 (22, 23) in the presence of 0.25% CHAPSO, and the production of A $\beta$ 40 was quantified using a G2-10 antibody (23).  $\gamma$ -Secretase activity was defined by the difference between signals obtained in the absence and the presence of L685,458 (L458), a potent  $\gamma$ -secretase inhibitor (24) (Fig. 2A). We now show that  $\gamma$ -secretase activity increases as a function of the amount of PS1 $\Delta$ E9-proteoliposomes (Fig. 2A) and that both L458 and compound E inhibited the activity of purified PS1 $\Delta$ E9 proteoliposomes at IC<sub>50</sub> values of 4.3 and 0.9 nM, respectively (Fig. S1B), values that are well within the known inhibitor profiles of the compounds with native  $\gamma$ -secretase complexes.

We then examined the accessibility of PS1 $\Delta$ E9 and PS1 $\Delta$ E9-D385A to an active-site directed probe JC-8, which has been shown to label active  $\gamma$ -secretase (25–27). We show that photoactivated JC-8 labels PS1 $\Delta$ E9 in proteoliposomes (Fig. 2B, lane 2) but not the inactive PS1 $\Delta$ E9-D385A mutant (Fig. 2B, lane 4). Furthermore, photoinsertion of JC-8 into PS1 $\Delta$ E9 is blocked by an excess of L458 (Fig. 2B, lane 1). Finally, to directly visualize the active  $\gamma$ -secretase, we have developed microsphere-supported assemblies combined with the activity-based probe for microscopic analysis. We have previously demonstrated that Compound 5 (Cpd 5) is capable of capturing active  $\gamma$ -secretase complexes under native conditions (28). We fused the PS1 $\Delta$ E9 proteoliposomes with silica microspheres to form assemblies in which the lipid bilayer is separated from the silica surface by a 1–2 nm water layer (29), and termed these PS1 $\Delta$ E9 proteolipobeads. Binding of Cpd 5 to the beads should mimic the assemblies as inhibitor- $\gamma$ -secretase bimolecular complex. Next, we added AlexaFluor®-633 conjugated streptavidin (AF633-SA) that binds to the biotin moiety positioned at the end of Cpd 5 assemblies to generate a tripartite complex (Fig. 2C). We imaged these assemblies using confocal laser-scanning microscopy (CLSM) and examined the 3D surface distributions of the AF633-SA from  $\Delta$ E9 or  $\Delta$ E9-D385A complexes present on single beads (Fig. 2C). The  $\Delta$ E9-microsphere complex showed significantly higher fluorescence intensity than the  $\Delta$ E9D385A-microsphere complexes (Fig. 2C). Additionally, the fluorescence is highly uniformly distributed in the AF633-SA- $\Delta$ E9 proteolipobeads, consistent with specific binding and localization of complex formation as compared to the heterogeneous nonspecific binding of AF633-SA to  $\Delta$ E9D385A proteolipobeads (Fig. 2C). Again, the PS1 $\Delta$ E9-proteolipobead CLSM study and the resulting images reveal that the active-site directed  $\gamma$ -secretase inhibitor specifically binds to the reconstituted PS1 $\Delta$ E9 but not to the catalytically dead form of PS1 $\Delta$ E9, findings that directly corroborate the earlier photo-labeling analyses (Fig. 2B). In addition, we also demonstrated that neither reconstituted PS1 $\Delta$ E9-D385A nor liposomes alone exhibit  $\gamma$ -secretase activity (Fig. 2D). Finally, we show that by directly incorporating the recombinant  $\Delta$ E9 and Sb4 substrates into liposomes, we observed  $\gamma$ -secretase activity in the absence of CHAPSO but not in liposomes containing incorporated recombinant  $\Delta$ E9-D385A and Sb4 (Fig. S1C). These findings establish that the reconstituted  $\gamma$ -secretase activity of PS1 $\Delta$ E9 is a bona fide property of the polypeptide and not generated by impurities present in the liposomes.

We next examined the production of A $\beta$ 40 and A $\beta$ 42 by proteoliposomes containing either PS1 $\Delta$ E9 or the PS1 $\Delta$ E9-C290S variant that is predicted to mimic the activity of wild-type PS1 (Fig. 2D). We show that in comparison to the PS1 $\Delta$ E9-C290S variant, the activity of the PS1 $\Delta$ E9 variant generated lower A $\beta$ 40 and elevated A $\beta$ 42 (Fig. 2D). These findings are consistent with studies in transfected HEK293 cells showing that expression of the FAD-linked PS1 $\Delta$ E9 variant leads to a decrease in steady-



activity of both preparations. From these values, we could calculate the specific activity of each preparation. We found that the specific  $\gamma$ -secretase activity of reconstituted  $\Delta E9$ -C290S is approximately 11% of the purified complex (Fig. S1E). These studies would suggest that other subunits of the complex may be required for maximal activity.

**Reconstituted PS1  $\Delta E9$  Processes APP Variants Leading to Elevated  $A\beta_{42}$ : $A\beta_{40}$  Ratios.** Earlier studies have shown that expression of FAD-linked mutations within the APP transmembrane domain leads to elevated ratios of  $A\beta_{42}$  to  $A\beta_{40}$  peptides in vivo (37, 38) and that coexpression of mutant PS1 variants acts synergistically to further elevate this ratio (33). Exploiting our reconstituted PS1 $\Delta E9$  proteoliposome  $\gamma$ -secretase assay, we analyzed the production of  $A\beta$  peptides derived from Sb4 substrates that harbor either the FAD-linked V46F mutation (39) or an experimental I45F mutation (numbering based on the  $A\beta$  sequence) that leads to an extremely high ratio of  $A\beta_{42}$ : $A\beta_{40}$  peptides (40, 41). Both the I45F and V46F substrates reduced the production of  $A\beta_{40}$  and significantly increased the generation of  $A\beta_{42}$  (Fig. 3D). The relative ratios of  $A\beta_{42}$ : $A\beta_{40}$  for WT-APP, I45F, and V46F were 0.28, 1.14, and 0.60, respectively (Fig. 3E), findings that recapitulate those obtained in studies performed both in transfected cells (41, 42) and in biochemical assays (40). These results confirm that the PS1 $\Delta E9$  proteoliposome exhibits the appropriate specificity for substrate cleavage and fully supports our earlier conclusion that PS1 $\Delta E9$ , in the absence of other components of the  $\gamma$ -secretase complex, is catalytically active as  $\gamma$ -secretase.

**Endoproteolytic "Activation" of PS1.** Our initial attempts to reconstitute  $\gamma$ -secretase activity with full-length PS1-MBP fusions were unsuccessful. We interpreted this result to suggest that full-length PS1 (PS1-FL) is an inactive zymogen, a view entirely consistent with our earlier discovery that PS1-FL overexpressed in mammalian cells fails to interact with a photoactivatable active-site directed inhibitor (18). On the other hand, PS1 lacking sequences encoded by exon 9 (PS1 $\Delta E9$ ) can clearly behave as an active enzyme despite the fact that it is not subject to endoproteolytic processing (18). In addition, previous studies showed that PS1 harboring an experimental M292D mutation that blocks endoproteolytic cleavage generates an active  $\gamma$ -secretase in mammalian cells (42). To test this PS1 variant in our reconstitution system, we expressed and purified the PS1-M292D-MBP fusion and assayed  $\gamma$ -secretase activity. We found that the uncleaved PS1-M292D possesses  $\gamma$ -secretase activity (Fig. S2A) and binds to JC-8 (Fig. S2B). These studies further support our conclusion that PS1 alone is catalytically active.

To establish a system that would enable endoproteolytic processing of the zymogen leading to "activation" of the enzyme. PEN-2 has been shown to play an essential role in PS1 endoproteolysis following binding to the NCT-Aph1-PS1 tertiary complex (3–5). To address the role of PEN2 in this process, we overexpressed and purified MBP-PEN2 from bacterial cells and coinorporated it together with PS1-FL into liposomes. Remarkably, we find that in proteoliposomes, PS1-FL is subject to endoproteolytic processing in the presence of PEN2 (Fig. 4A, Upper, lane 2) but not in its absence (Fig. 4A, Upper, lane 1). The existence of PEN2 in the proteoliposomes was confirmed by Western blotting (Fig. 4A, Lower). Most importantly, we now document that the PEN2-mediated endoproteolytic "activation" of PS1 gives rise to  $\gamma$ -secretase activity (Fig. 4B), a property not observed in liposomes containing only full-length PS1 or PEN2. Importantly, the photoactivatable probe, JC-8, only labels the newly generated PS1-NTF but not PS1-FL or other species present in the reaction (Fig. 4C), thus further supporting the view that the active form of  $\gamma$ -secretase requires endoproteolytic processing of PS1 to generate amino- and carboxyl-terminal fragments. Taken together, our in vitro reconstitution system faithfully recapitulates the essential

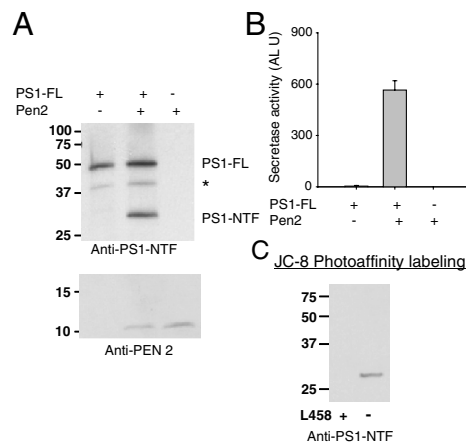


**Fig. 4.** Proteoliposome containing both full-length PS1 and PEN2 proteins exhibits  $\gamma$ -secretase activity. (A) Western analysis with PS1 NTF and PEN2 antibodies. Proteoliposome containing both PS1 and PEN2 shows a specific band corresponding to PS1 NTF. \* Breakdown product of unknown identity. (B) Proteoliposome containing both PS1 and PEN2 displayed  $\gamma$ -secretase activity.  $\gamma$ -Secretase activity was measured by G2-10 antibody that recognizes with  $A\beta_{40}$  with AlphaLISA technology. (C) The PS1-NTF was specifically labeled by JC-8, but not PS1-FL in the PS1 + PEN2 liposome. Furthermore, this labeling was blocked by L458.

biochemical and molecular features of  $\gamma$ -secretase activation that has heretofore only been observed in living cells. Moreover, our studies reveal that PEN2 plays an obligatory role in the activation of PS and does so in the absence of other subunits of the complex.

## Discussion

The roles of APH-1, NCT, and PEN2 in trafficking, stabilization, assembly, and maturation of the  $\gamma$ -secretase complex have been extensively documented, and it is a widely held view that PS is the catalytic subunit. However, the role of individual subunits in promoting catalysis and cleavage site specificity are largely unknown and confounded by the fact that in mammalian cells,  $\gamma$ -secretase activity requires the expression of all four subunits. In the present study, we have tested the proposal that PS, absent other components of the complex, can exhibit  $\gamma$ -secretase catalysis and cleavage specificity and now offer several important insights. First, we demonstrate that proteoliposomes containing PS1 $\Delta E9$  or PS1M292D, alone, are sufficient to catalyze  $\gamma$ -secretase processing of APP and Notch1 substrate. Second, we show that the ratio of  $A\beta_{42}$ / $A\beta_{40}$  peptides of approximately 10% generated in proteoliposomes containing a wild-type PS1 molecule is elevated to approximately 20% in proteoliposomes containing the FAD-linked PS1 $\Delta E9$  variant, findings consistent with observations in in vivo settings wherein all four components of the complex are expressed. Finally, we demonstrate that PS1 $\Delta E9$  proteoliposomes alter the cleavage specificity within the transmembrane domain of mutant APP substrates leading to elevated  $A\beta_{42}$ / $A\beta_{40}$  ratios in a manner that reflects the findings in in vivo settings. Collectively, these results provide compelling proof that PS is sufficient for  $\gamma$ -secretase activity and specificity to generate varying levels of  $A\beta_{40}$  and  $A\beta_{42}$ .

To the insights arising from our proteoliposome reconstitution assays of  $\gamma$ -secretase, we have established the utility of our assay to understand the essential biochemical requirements for endoproteolytic activation of the PS1 zymogen. While earlier efforts have indicated that PEN2 facilitates the endoproteolysis upon association with the fourth transmembrane domain of PS1 (43), there is presently no information to suggest that PEN-2 acts alone or in collaboration with other subunits of the complex that are coexpressed in living cells. We now demonstrate that PEN2, alone, is both necessary and sufficient to promote endoproteolysis and catalytic activation of PS1. By inference, we suggest that PEN2 facilitates the conversion of PS1-FL into a PSase-competent form

that promotes autocatalysis. However, the contribution of PEN2 in mediating catalysis remains to be investigated. Taken together, these reconstitution studies strongly suggest that the bimolecular interaction of PS1 and PEN2 induces PSase activity and the processed derivatives of PS1 exhibit  $\gamma$ -secretase activity.

Our studies now confirm the earlier proposal that PS1-FL is an inactive zymogen (18). We now offer several models that support our experimental evidence for  $\gamma$ -secretase activation (Fig. 5): First, PEN2 interacts with PS1 to facilitate the intrinsic PSase activity; second, the PS1 $\Delta$ E9 variant is constitutively active because an “autoinhibitory” domain is removed, consistent with an earlier proposal (44). In this regard, studies by Fukumori et al. (12) suggested that the autoinhibitory domain “plugs” the catalytic site into a “closed” conformation that does not allow substrate access. Alternatively, we propose that the autoinhibitory domain interferes with the appropriate positioning and/or orientation of the catalytic aspartyl dyad necessary for catalysis rather than directly affecting substrate access to the catalytic site(s). In support of this model, unprocessed catalytically inactive PS1-FL harboring D257A or D385A mutations can still bind to substrates (45) but not JC-8. In either model, deletions and/or endoproteolytic cleavage within the autoinhibitory domain removes the constraints imposed by this region, leading to generation of an active form of the enzyme. With the same reasoning, we propose that the insertion of a charged aspartate residue in the PS1-M292D molecule leads to activation.

In summary, we have established a reconstitution platform that has allowed us to conclusively demonstrate that PS1 is  $\gamma$ -secretase and PEN2 is required for the activation of PS1. It will be essential to reconstitute the entire complex using the proteoliposome platform, described herein, in order to examine the contributions of each component either individually or in combination with PS1 in mediating intramembranous proteolysis. This system provides an entirely unique approach to elucidate the reaction mechanism of  $\gamma$ -secretase at both molecular and atomic levels, with the expectation that these efforts will lead to the development of effective therapies for AD and human malignancies in which  $\gamma$ -secretase/Notch signaling plays a central role.

## Materials and Methods

**Reagents.** All lipids in this study were purchased from Avanti Polar Lipids, Inc. L458, compound E, and JC-8 were synthesized in our laboratory (25, 28).

**Expression and Purification of Recombinant PS1 $\Delta$ E9 and Mutants.** cDNA encoding PS1 $\Delta$ E9 and other PS1 variants were cloned into the pIAD16 vector for

protein expression and purification (19). Each protein was expressed in BL21(DE3) cells, and IPTG was added to the culture at a final concentration of 0.1 mM when bacterial cell density reached an OD<sub>600</sub> of approximately 0.5–0.6. The bacteria were further cultured at 20 °C for 5 h then harvested and resuspended in 20 mM Tris, 150 mM NaCl, pH7.4 buffer. Following lysis using a French press, the lysate was centrifuged for 1 hr at 100,000 g, 4 °C, and the supernatant fraction was loaded into an amylose column and eluted with a gradient of maltose.

**Preparation of Liposome.** Medium-sized Unilamellar Vesicles (MUVs, 100 nm) were prepared from mixtures of lipids using extrusion. Lipids were mixed as CHCl<sub>3</sub> solutions in a round-bottomed flask, dried as a thin film under reduced pressure in a rotary evaporator for 20 min, and evacuated under high vacuum for 2 h. The lipid film was resuspended in 5 mL of buffer (20 mM Tris, 150 mM NaCl, 10 mM MgCl<sub>2</sub>, pH7.4). The resuspended mixture was frozen at –80 °C in liquid nitrogen and thawed at 65 °C in a water bath, a procedure repeated five times. MUV was prepared by 10 extrusion cycles using an extruder. For this, the resuspended material was passed through two stacked 100-nm filters using a nitrogen gas pressure of 350–400 psi, thus producing a homogeneous batch of liposomes.

**Preparation of Proteoliposomes.** A freshly prepared batch of MUV was mixed with CHAPS at a 1:2 lipid:detergent ratio (w/w) and incubated end over end at 4 °C for 1 hr. PS1-MBP-fused target proteins were added to the liposome-detergent mixture at 1:50 or 1:100 protein:lipid ratio (w/w) and end over end incubation at 4 °C for 1–2 hr. Detergent removal was initiated by incubation with SM-2 bead (120–150 mg/each cycle) at 4 °C for 2 hr, followed by dialysis for 8 hr at 4 °C. Cleavage of the MBP portion was performed by incubation with thrombin for 3–6 h at 16 °C. The reaction was terminated by addition of a thrombin inhibitor. Isolation and concentration of proteoliposomes was achieved via gradient sucrose centrifugation. The dialysates (600  $\mu$ l) were mixed with 600  $\mu$ l of 80% (w/v) sucrose solution and added to 12 mL ultracentrifugation tubes. Seven sucrose layers (800  $\mu$ l each) with sucrose concentrations (37.0%, 32.5%, 29.5%, 21.0%, 17.2%, 13.4%, and 9.0% in buffer) were carefully added to the tube and centrifuged to 16,000 g at 4 °C for 3 h. Proteoliposomes were collected from the top layer. The protein concentration in the proteoliposomes was determined using DC Protein assay kit.

**In vitro  $\gamma$ -Secretase Assay with Proteoliposomes.** In vitro  $\gamma$ -secretase activity assays were similar to those described previously (22, 40, 46). Briefly, the Sb4 was incubated with proteoliposomes in the presence of 0.25% CHAPSO. The reaction mixtures were then incubated with G2-10 or G2-11 antibodies, which specifically recognize A $\beta$ 40 and A $\beta$ 42 peptides, and detected by electrochemiluminescence (ECL) or AlphaLISA (AL) signals. Thus, the activity was expressed as the ECL U or AL U, respectively.  $\gamma$ -Secretase activity for Notch1 was measured using anti-NICD antibody with AlphaLISA technology. All data were analyzed with Student's *t* test by the KaleiaGraph program. The statistical difference was indicated by *p*-values (*p*-values: \* <0.05; \*\* <0.01; \*\*\* <0.001).

**Photolabeling of PS1 $\Delta$ E9 Proteoliposome.** The procedure similar to that described earlier (18, 26, 27) was used to photo-crosslink JC-8 and targets in proteoliposomes. Fresh proteoliposomes (600  $\mu$ l) containing various PS1 variants in the presence of 0.25% CHAPSO were preincubated with or without L458 (1  $\mu$ M) at 37 °C for 30 min. The compound JC-8 (10 nM) was added and incubated at 37 °C for 1 hr. Following UV irradiation, JC-8-crosslinked proteins were isolated using streptavidin beads and bound proteins were analyzed by Western blotting using a PS1-NTF specific antibody.

**Immobilized  $\gamma$ -Secretase Proteoliposome Assays.** Purified PS1  $\Delta$ E9 proteoliposomes were fused with 4.74  $\mu$ m nominal size silica microspheres for 30 min at a ratio of greater than 10:1 lipid bilayer area to total microsphere surface area, followed by four wash steps to remove excess proteoliposomes. After PS1 $\Delta$ E9-proteolipobeads were incubated with Cpd 5 and AlexaFluor633-labeled streptavidin (AF633-SA) and washed, confocal microscopy was used to image AF633-SA bound to the surface of the proteolipobead assemblies. Samples were imaged using a Leica TCS SP2 AOB5 Confocal Microscope System equipped with argon ion and HeNe lasers. A 63X/1.4 NA oil immersion objective was used for all the images. Alexa Fluor 633 was excited using 633 nm line of a He/Ne laser, and images were taken with the detection window set between 645–750 nm. Samples were compared under the same detector and laser settings in adjacent wells sharing the same coverglass by employing eight-well Lab-Tek II #1.5 chambered coverglasses. The 3D recon-

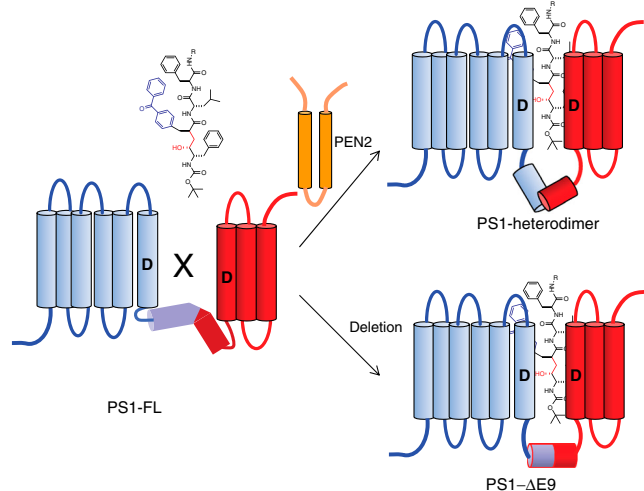


**Fig. 5.** The proposed activation mechanism of PS1. PS1-FL is considered as a zymogen for proteolysis and active-site-directed inhibitor binding. Endoproteolysis and deletion at exon 9 convert PS1-FL into the active enzyme. Exon 9 can serve a steric constraint for positioning the two catalytic Asp residues.

struction of XY Z-stacks was obtained using ImageJ 1.4.1 f with the 3D Viewer plugin.

**ACKNOWLEDGMENTS.** This work is supported by National Institutes of Health Grant AG026660 (Y.M.L.), the Alzheimer's Association (Y.M.L.), the American

Health Assistance Foundation (Y.M.L.), Mr. William H. Goodwin and Mrs. Alice Goodwin and the Commonwealth Foundation for Cancer Research, the Experimental Therapeutics Center of Memorial Sloan-Kettering Cancer Center, the William Randolph Hearst Fund in Experimental Therapeutics (Y.M.L.), Cure Alzheimer's Fund (S.S.S.), and the Adler Foundation (S.S.S.).

1. De Strooper B (2003) Aph-1, Pen-2, and nicastrin with presenilin generate an active gamma-secretase complex. *Neuron* 38:9-12.
2. Edbauer D, et al. (2003) Reconstitution of gamma-secretase activity. *Nat Cell Biol* 5:486-488.
3. Thinakaran G, et al. (1996) Endoproteolysis of presenilin 1 and accumulation of processed derivatives in vivo. *Neuron* 17:181-190.
4. Takasugi N, et al. (2003) The role of presenilin cofactors in the gamma-secretase complex. *Nature* 422:438-441.
5. Luo WJ, et al. (2003) PEN-2 and APH-1 coordinately regulate proteolytic processing of presenilin 1. *J Biol Chem* 278:7850-7854.
6. Zhang YW, et al. (2005) Nicastrin is critical for stability and trafficking but not association of other presenilin/gamma-secretase components. *J Biol Chem* 280:17020-17026.
7. Kim SH, Ikeuchi T, Yu C, Sisodia SS (2003) Regulated hyperaccumulation of presenilin-1 and the "gamma-secretase" complex. Evidence for differential intramembranous processing of transmembrane substrates. *J Biol Chem* 278:33992-34002.
8. Shah S, et al. (2005) Nicastrin functions as a gamma-secretase-substrate receptor. *Cell* 122:435-447.
9. Chavez-Gutierrez L, et al. (2008) Glu(332) in the Nicastrin ectodomain is essential for gamma-secretase complex maturation but not for its activity. *J Biol Chem* 283:20096-20105.
10. Zhao G, Liu Z, Ilagan MX, Kopan R (2010) Gamma-secretase composed of PS1/Pen2/Aph1a can cleave notch and amyloid precursor protein in the absence of nicastrin. *J Neurosci* 30:1648-1656.
11. Wolfe MS, et al. (1999) Two transmembrane aspartates in presenilin-1 required for presenilin endoproteolysis and gamma-secretase activity. *Nature* 398:513-517.
12. Fukumori A, Fluhrer R, Steiner H, Haass C (2010) Three-amino acid spacing of presenilin endoproteolysis suggests a general stepwise cleavage of gamma-secretase-mediated intramembrane proteolysis. *J Neurosci* 30:7853-7862.
13. Campbell WA, Reed ML, Strahle J, Wolfe MS, Xia W (2003) Presenilin endoproteolysis mediated by an aspartyl protease activity pharmacologically distinct from gamma-secretase. *J Neurochem* 85:1563-1574.
14. Nyabi O, et al. (2003) Presenilins mutated at Asp-257 or Asp-385 restore Pen-2 expression and nicastrin glycosylation but remain catalytically inactive in the absence of wild type presenilin. *J Biol Chem* 278:43430-43436.
15. De Strooper B, et al. (1998) Deficiency of presenilin-1 inhibits the normal cleavage of amyloid precursor protein. *Nature* 391:387-390.
16. Naruse S, et al. (1998) Effects of PS1 deficiency on membrane protein trafficking in neurons. *Neuron* 21:1213-1221.
17. Eslser WP, et al. (2000) Transition-state analogue inhibitors of gamma-secretase bind directly to presenilin-1. *Nat Cell Biol* 2:428-434.
18. Li YM, et al. (2000) Photoactivated gamma-secretase inhibitors directed to the active site covalently label presenilin 1. *Nature* 405:689-694.
19. Lei X, Ahn K, Zhu L, Ubarretxena-Belandia I, Li YM (2008) Soluble oligomers of the intramembrane serine protease YqgP are catalytically active in the absence of detergents. *Biochemistry* 47:11920-11929.
20. Ikeuchi T, Dolios G, Kim SH, Wang R, Sisodia SS (2003) Familial Alzheimer disease-linked presenilin 1 variants enhance production of both Abeta 1-40 and Abeta 1-42 peptides that are only partially sensitive to a potent aspartyl protease transition state inhibitor of "gamma-secretase". *J Biol Chem* 278:7010-7018.
21. Steiner H, et al. (1999) The biological and pathological function of the presenilin-1 Deltaexon 9 mutation is independent of its defect to undergo proteolytic processing. *J Biol Chem* 274:7615-7618.
22. Shelton CC, Tian Y, Frattini MG, Li YM (2009) An exo-cell assay for examining real-time gamma-secretase activity and inhibition. *Mol Neurodegener* 4:22.
23. Tian Y, Crump CJ, Li YM (2010) Dual role of {alpha}-secretase cleavage in the regulation of {gamma}-secretase activity for amyloid production. *J Biol Chem* 285:32549-32556.
24. Shearman MS, et al. (2000) L-685,458, an aspartyl protease transition state mimic, is a potent inhibitor of amyloid beta-protein precursor gamma-secretase activity. *Biochemistry* 39:8698-8704.
25. Chun J, Yin Yi, Yang G, Tarassishin L, Li YM (2004) Stereoselective synthesis of photo-reactive peptidomimetic gamma-secretase inhibitors. *J Org Chem* 69:7344-7347.
26. Shelton CC, et al. (2009) Modulation of gamma-secretase specificity using small molecule allosteric inhibitors. *Proc Natl Acad Sci USA* 106:20228-20233.
27. Tian Y, Bassit B, Chau D, Li YM (2010) An APP inhibitory domain containing the Flemish mutation residue modulates gamma-secretase activity for Abeta production. *Nat Struct Mol Biol* 17:151-158.
28. Placanica L, Zhu L, Li YM (2009) Gender- and age-dependent gamma-secretase activity in mouse brain and its implication in sporadic Alzheimer disease. *PLoS ONE* 4:e5088.
29. Bayerl TM, Bloom M (1990) Physical properties of single phospholipid bilayers adsorbed to micro glass beads. A new vesicular model system studied by 2H-nuclear magnetic resonance. *Biophys J* 58:357-362.
30. Kumar-Singh S, et al. (2006) Mean age-of-onset of familial Alzheimer disease caused by presenilin mutations correlates with both increased Abeta42 and decreased Abeta40. *Hum Mutat* 27:686-695.
31. Steiner H, et al. (2000) Glycine 384 is required for presenilin-1 function and is conserved in bacterial polytopic aspartyl proteases. *Nat Cell Biol* 2:848-851.
32. Moehlmann T, et al. (2002) Presenilin-1 mutations of leucine 166 equally affect the generation of the Notch and APP intracellular domains independent of their effect on Abeta 42 production. *Proc Natl Acad Sci USA* 99:8025-8030.
33. Citron M, et al. (1998) Additive effects of PS1 and APP mutations on secretion of the 42-residue amyloid beta-protein. *Neurobiol Dis* 5:107-116.
34. Levitan D, et al. (2001) PS1 N- and C-terminal fragments form a complex that functions in APP processing and Notch signaling. *Proc Natl Acad Sci USA* 98:12186-12190.
35. Bentahir M, et al. (2006) Presenilin clinical mutations can affect gamma-secretase activity by different mechanisms. *J Neurochem* 96:732-742.
36. Kounnas MZ, et al. (2010) Modulation of gamma-secretase reduces beta-amyloid deposition in a transgenic mouse model of Alzheimer's disease. *Neuron* 67:769-780.
37. Borchelt DR, et al. (1996) Familial Alzheimer's disease-linked presenilin 1 variants elevate Abeta1-42/1-40 ratio in vitro and in vivo. *Neuron* 17:1005-1013.
38. Scheuner D, et al. (1996) Secreted amyloid beta-protein similar to that in the senile plaques of Alzheimer's disease is increased in vivo by the presenilin 1 and 2 and APP mutations linked to familial Alzheimer's disease. *Nat Med* 2:864-870.
39. Suzuki N, et al. (1994) An increased percentage of long amyloid beta protein secreted by familial amyloid beta protein precursor (beta APP717) mutants. *Science* 264:1336-1340.
40. Yin Yi, et al. (2007) {gamma}-secretase substrate concentration modulates the Abeta42/Abeta40 ratio: Implications for Alzheimer disease. *J Biol Chem* 282:23639-23644.
41. Lichtenthaler SF, et al. (1999) Mechanism of the cleavage specificity of Alzheimer's disease gamma-secretase identified by phenylalanine-scanning mutagenesis of the transmembrane domain of the amyloid precursor protein. *Proc Natl Acad Sci USA* 96:3053-3058.
42. Steiner H, et al. (1999) Amyloidogenic function of the Alzheimer's disease-associated presenilin 1 in the absence of endoproteolysis. *Biochemistry* 38:14600-14605.
43. Kim SH, Sisodia SS (2005) Evidence that the "NF" motif in transmembrane domain 4 of presenilin 1 is critical for binding with PEN-2. *J Biol Chem* 280:41953-41966.
44. Knappenberger KS, et al. (2004) Mechanism of gamma-secretase cleavage activation: Is gamma-secretase regulated through autoinhibition involving the presenilin-1 exon 9 loop? *Biochemistry* 43:6208-6218.
45. Xia W, et al. (2000) Presenilin complexes with the C-terminal fragments of amyloid precursor protein at the sites of amyloid beta-protein generation. *Proc Natl Acad Sci USA* 97:9299-9304.
46. Li YM, et al. (2000) Presenilin 1 is linked with gamma-secretase activity in the detergent solubilized state. *Proc Natl Acad Sci USA* 97:6138-6143.